Image Interpolation Based on Weighted and Blended Rational Function

Yifang Liu, Yunfeng Zhang, Qiang Guo, Caiming Zhang

School of Computer Science and Technology, Shandong University of Finance and Economics, Jinan 250014, China;
Shandong Provincial Key Laboratory of Digital Media Technology, Jinan 250014, China
yfzhang@sdufe.edu.cn

Abstract. Conventional linear interpolation methods produce interpolated images with blurred edges, while edge directed interpolation methods make enlarged images with good quality edges but with details distortion for some cases. An adaptive rational-based algorithm for the interpolation of digital images with arbitrary scaling factors is proposed. In order to remove artifacts, we construct a new interpolation model with weight and blend, which are used for preserving the clear edge and detail. The proposed model is blended by basic rational interpolation model and three rotated rational models. The weight coefficients are determined by the edge information from different scale based on point sampling. Experimental results show that the proposed method produces images with high objective quality assessment value and good visual quality.

1 Introduction

Image interpolation has a wide range of applications which aims to reconstruct a high resolution (HR) image from the low-resolution (LR) image. The most common interpolation methods are bilinear, bicubic, cubic spline algorithm, etc [6, 3]. These conventional methods are the approximation of sinc function which corresponds to ideal filtering [14]. These methods have a relatively low complexity, but suffer from several types of visual degradation around "edges".

To solve these problems, many adaptive interpolation algorithms have been developed [2, 4, 7–10, 13, 15–18]. These algorithms can be broadly divided into two categories: discrete method and continuous method. In discrete method, new edge-directed interpolation (NEDI)[8]estimates high resolution covariances form low resolution image based on the geometric duality; In [17], for a pixel to be interpolated two observation sets are defined in two orthogonal directions, and then fuse the directional interpolation results by minimum mean square-error estimate; Zhang and Wu [18] develop a soft-decision interpolation method which is able to estimate missing pixels by groups instead of by pixels. These discrete algorithms which consider more adaptive image information can improve the visual effect. However, these methods deliver not a continuous function but a set of subpixel values which are not suitable for resampling after, for example, rotation

[10], and they have a much higher computational complexity than conventional methods. Besides, these methods sometimes generate speckle noise or distortion of edges[18].

Once a digital image is converted into an interpolating continuous function, we can resample it to obtain resized and rotated images at a better precision [10]. In fact, the continuous methods create a HR image though constructing a interpolating patch. [4] presents a method for preserving the contours or edges based on adaptive osculatory rational interpolation kernel function. [16] constructs a fitting surface by using image data as constraints to reverse sampling process for improving fitting precision. However, these continuous methods all suffer form blurred edge in some ways. Recently, a bivariate rational interpolation with parameters based on the function values is studied in [19, 12]. The rational function has a simple and explicit expression, and compared with other methods, it can keep the natural attributes of image better. Because the rational model is suitable for resizing natural image, it performs the details well and a relative clear edge. Unfortunately, the single bivariate rational model(basic model (Fig.2a)) is asymmetric and does not meet the structures of natural image. So it can produce zigzagging artifacts around the edge regions.

In this paper, we construct an adaptive interpolation function with weight and blend based on rational function model. To reduce the zigzagging edge generated by the basic model, we rotate the basic rational model 3 times to get 4 interpolating functions. The proposed model is weighted and blended by them. The weight coefficients which contain edge information are adaptively calculated by distance, gradient and difference quotient based on point sampling, and can be used to keep the edge attributions. Experiments show that the proposed approach performs better than conventional and discrete methods in preserving edge.

This paper addresses the problem of constructing an adaptive weighted rational function such that the resized image has better precision and visual quality. We use blending model not only to maintain the image natural attribution but also to preserve the structure of image, and the adaptive weight coefficients can preserve edge information from different aspects. Furthermore, point sampling can ensure that more information in a cell can be used to determined the weight coefficients.

The paper is arranged as follows. In Section 2, the proposed interpolated model based on basic rational model is introduced. Section 3 shows the performance of the method.

2 Description of proposed method

In this section, the interpolation function with unknown weight coefficients is proposed, and the key problem is to determine the weight coefficients. Then the weight coefficients are determined by different scale edge information of local image.

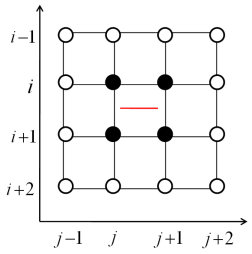

Fig. 1. The interpolation model

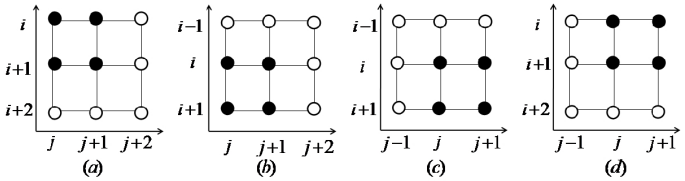

Fig. 2. The rotation model: (a)Basic model; (b), (c) and (d) are 90, 180 and 270 degree counterclockwise rotation of (a) respectively.

2.1 The interpolation model

Thought rational function has good features to maintain details, it suffers from some visual problems around edge region. The proposed model can preserve edge region well as well as detail region. Let $[i, i+1; j, j+1]$ be the interpolated region. The proposed interpolation model based on rational spline function is showed in Fig.1. The rectangle region surrounded by 4 black points is the interpolated region. All 16 points within the interpolation model are involved in the interpolation. And Fig.2 shows the decomposition of the proposed model. The proposed model is weighted and blended by the 4 submodels. In Fig.2, (a) means the basic rational spline interpolation model; (b) represents the 90 degree counterclockwise rotation of (a) in Fig.1 model, and the rotation center is the interpolation region; in the same way, (c) and (d) are 180 and 270 degree counterclockwise of (a). Fig.3 is another expression of Fig.2, and (a), (b), (c) and (d) correspond respectively. Let the basic rational spline interpolation model (a) denotes $P_1(x, y)$, then (b), (c) and (d) are denoted $P_2(1-y, x)$, $P_3(1-x, 1-y)$ and $P_4(y, 1-x)$ respectively. All these four submodels can produce the same patch $[i, i+1; j, j+1]$. The proposed weighted and blended rational function $P_{i,j}(x, y)$ is expressed in Eq.1.

$$\begin{aligned} P_{i,j}(x,y) &= aP_1(x,y) + bP_2(1-y,x) \\ &+cP_3(1-x,1-y) + dP_4(y,1-x), \end{aligned} \tag{1}$$

where a, b, c and d are unknown weight coefficients.

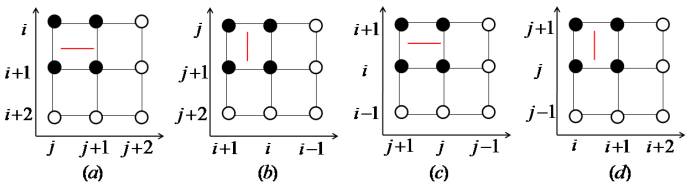

Fig. 3. The rotation model: (a)$P_1(x, y)$; (b)$P_2(1-y, x)$; (c)$P_3(1-x, 1-y)$; (d)$P_4(y, 1-x)$.

Now the basic rational spline function (Fig.2(a)) is given. A bivariate rational interpolation with parameters based on the function values is constructed in [19, 12]. Let $P_{i,j}(x, y)$ be a bivariate function defined in the region $[i, i+1; j, j+1]$. Denote the pixel value by $I_{i,j}$. For any point $(x, y) \in [i, i+1; j, j+1]$, the bivariate rational interpolating function $P_{i,j}(x, y)$ can be expressed as

$$P_{i,j}(x, y) = \sum_{r=0}^{2} \sum_{s=0}^{2} \omega_r(x, \alpha_i)\omega_s(y, \beta_j) I_{i+r,j+s}, \tag{2}$$

where

$$\omega_0(t, \delta) = \frac{(1-t)^2(\delta + t)}{(1-t)\delta + t},$$
$$\omega_1(t, \delta) = \frac{t(1-t)\delta + 3t^2 - 2t^3}{(1-t)\delta + t},$$
$$\omega_2(t, \delta) = \frac{-t^2(1-t)}{(1-t)\delta + t}.$$

Considering the basic model, 9 points $I_{i+r,j+s}$,$(r, s = 0, 1, 2)$ are used to construct the patch $P_1(x, y)$ which crosses the 4 black points, and these 9 points have different basis functions. However, it would suffer from blurred edges. There are two main reasons. On the one hand, for a nature image, it will result some artifacts around edges because of its asymmetry; on the other hand, the function is constructed by x-direction first and then y-direction, which results the advantage on x-direction [19]. The proposed weighted and blended interpolation model can refrain from these two factors. Obviously, Fig.1 contains 16 points and the interpolated region is located in the center of the model. And it is easy to know that the disadvantage of y-direction is eliminated through the rotation. For example, there is a horizontal direction edge marked in red as shown in Fig.1. And Fig.3 shows the changes of the direction of the red edge during rotation. We can see that in (a) and (c), the red edge is still horizontal, while it rotates to vertical direction in (b) and (d) models. It means that the proposed interpolation model balances the effect of different edge directions.

Then the edge information is used as constraints to determine the weight coefficients. It would not only be able to ensure good visual perception of detail areas, but also make the edge regions avoid zigzagging.

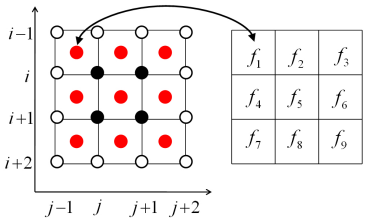

Fig. 4. Every cell can be regard as a point.

2.2 Adaptive weights

From discussed above, we know that the weight coefficients are vital to the interpolation effect. And the weight coefficients should reflect local structure information and natural attributions of image. Following, the determination of the unknown in Eq.1 is discussed. Adaptive interpolation means that the way the neighboring pixels influence the value of the interpolated pixel depends on local properties [11]. Thus the weight coefficients should be different when the construction of near pixels is different. In the proposed model, the 4×4 pixels region is divided into 4 overlapping subregions, and the contribution of each subregion to the intermediate patch determines the weight coefficients. The 1×1 rectangular region composed of four pixels can be seen as a basic cell. It can be seen from Fig.4 that every subregion can be regraded as four basic cells, then the whole interpolation model contains 9 cells denoted as $f_s, (s = 1, \cdots, 9)$. If we know the relationship between the 8-connected neighbors cells and intermediate cell f_5, it is easy to determine the four weight coefficients in Eq.1.

For all $s = 1, 2, 3, 4, 6, 7, 8, 9$, let w_s represent the impact factors between the patch f_s and f_5. In Fig.4, intuitively, f_5, f_6, f_8 and f_9 constitute the subregion P_1, and f_5 is the interpolated region. Thus we consider the relationship between f_6, f_8, f_9 and f_5 determines the contribution of the subregion P_1 to the intermediate interpolated region. And other subregions are in similar way. Then the a, b, c and d can be expressed as follows:

$$\begin{aligned} a = \frac{w_6 + w_8 + w_9}{W}, b = \frac{w_2 + w_3 + w_6}{W}, \\ c = \frac{w_1 + w_2 + w_4}{W}, d = \frac{w_4 + w_7 + w_8}{W}, \end{aligned} \tag{3}$$

where $W = w_1 + w_2 + w_7 + w_9 + 2w_2 + 2w_4 + 2w_6 + 2w_8$, which means normalization of the weight coefficients.

Now we discuss how to determine w_s. It is not easy to measure the relationship between two patches, while there are more approaches to measure the relationship between two points. Therefore a cell is regarded as a point such that the relationship between two cells can be approximately replaced by two points. Usually the pixel value can be regarded as the sample value of a continuous

patch[16]. The approximate point sampling value of a cell is expressed as

$$\iint_{A_{ij}} P_{i,j}(x,y)dxdy = \overline{P_{ij}} \times S_{ij},$$

where A_{ij} is a cell region, and S_{ij} is the area of A_{ij}, $P_{i,j}(x,y)$ represents function of a patch. Thus the point sampling value of patch can be approximately achieved by $\overline{P_{ij}}$. And the point values of f_1 to f_9 can be calculated. It is converted to a problem of computing the relationship between the intermediate point and the 8-connected neighbors points respectively.

In a natural image, distance, gradient and different quotient can measure the relationship between different pixels from different attributions. The *distance* measures the pixel space relationship, and the local *gradient* shows the edge information in a cell, and the *difference quotient* indicates the edge information among the whole model region. Thus, the local *gradient* and *difference quotient* can describe the edge from different scale. We focus on three factors *distance*, *gradient*, and *difference quotient* to determine the w_s, as shown in Eq.4

$$w_s = F(\textit{distance}, \textit{gradient}, \textit{difference quotient}). \tag{4}$$

Based on the weight expression of bilateral filter which contains distance and gray value, we construct a trilateral weighted expression. For all $s = 1, 2, 3, 4, 6, 7, 8, 9$, the Eq.4 can be represented as

$$w_s = e^{-\frac{w_s^1}{h_1^2}} \times e^{-\frac{w_s^2}{h_2^2}} \times e^{-\frac{w_s^3}{h_3^2}}, \tag{5}$$

where w_s^1, w_s^2 and w_s^3 represent *Distance*, *Gradient*, and *Difference Quotient* respectively, and h_1,h_2 and h_3 are adjusting parameters. Then the unknown w_s^1, w_s^2 and w_s^3 are calculated.

First, the weight coefficients depend on the distance between each point and the intermediate point. If f_s is closer to the intermediate point, the weight coefficient will be greater. It is shown as

$$w_s^1 = (x_5 - x_s)^2 + (y_5 - y_s)^2, \tag{6}$$

where x and y are the local coordinates of these points.

Second, the weight coefficients also depend on the local gradients. The local gradient is expressed as

$$w_s^2 = |f_x'|^2 + |f_y'|^2, \tag{7}$$

where the f_x' and f_y' are the local gradient of a cell around the interpolation patch. In essence the smaller the local gradient of a pixel is, the more influence it should have on the intermediate pixel[11]. Obviously, the small scale edge information is considered due to the gradients as one of the factors in a cell.

Third, the second difference quotient is taken into account. If there is an edge along the vertical direction, f_2 and f_8 should have the closest connection to f_5. They are defined as

$$w_2^3 = |2f_5 - f_2 - f_8|^2, \tag{8}$$

w_1^3, w_3^3 and w_4^3 are defined in the same way. And $w_6^3 = w_4^3$, $w_7^3 = w_3^3$, $w_8^3 = w_2^3$, $w_9^3 = w_1^3$. This factor reflects the large scale edge information in the whole region of 4×4, and the smaller the $w_{s,3}$ is, the more effect it should have on the f_5.

All the unknown factors are calculated. Substituting Eq.5 into Eq.3 gets the adaptive weights. Since the quality around the edges plays an important role in the visual effect of an image, $P_{i,j}(x, y)$ should reflect the characteristics around the edges as well as possible. In Eq.7, the local gradient which infers the local small scale edge is involved, and in Eq.8 all the pixels in the whole window are contained to determine weight coefficients which means that the large scale edge is considered. Thus the final weight coefficients a, b, c and d are adaptive by edge.

3 Experiments

The proposed method is compared with recent interpolation algorithms: new edge-directed interpolation (NEDI)[8], soft-decision interpolation (SAI)[18], sparse mixing estimators (SME)[9] and robust soft-decision interpolation (RSAI) [5]. All experiments are performed with softwares provided by the authors of these algorithms[1]. We have used 7 images as our benchmark images (Fig.5). We downsmaple these HR images to get the corresponding LR images. Table 1 gives the PSNRs and SSIMs generated by all algorithms for the images in Fig.5. It can be seen that the proposed method has a highest average PSNR and SSIM among all the algorithms.

Fig. 5. Benchmark images.

Fig.6-9 compare the interpolated images obtained by different algorithms. These images are cropped by red rectangle in Fig.5. Fig.8 shows the edge information, and the others show details. For Fig.8, all the algorithms perform similar results in edge region. We can see that NEDI suffers from some noisy interpolation artifacts (Fig.7,9,6(b) because of the fixed interpolation window. And SAI method also suffers from noisy artifacts in Fig.9(d) and Fig.6(d). RSAI performs better than SAI but produces some unconnected stripes (Fig.7(e) and Fig.6(e)). Although SME has similar visual quality with the proposed method, the objective quality assessment value is lower than the proposed algorithm. Therefore, the proposed method can keep the edge region well, and it can perform better detail areas than other algorithms. Moreover, we also compared the proposed method with the methods in papers DFDF [17], KR [13], INEDI [1],

[1] The source code of the proposed method is opened, please request the first author.

Table 1. PSNR and SSIM results of the reconstructed HR images.

Method	NEDI		SME		SAI		RSAI		Proposed	
	PSNR	SSIM	PSNR	SSIM	PSNR	SSIM	PSNR	SSIM	PSNR	SSIM
Barbara	22.36	0.8513	23.98	0.8731	23.55	0.8638	23.37	0.8618	**24.51**	**0.8795**
Fence	19.82	0.6853	21.47	0.7314	20.82	0.7182	21.556	0.7353	**21.56**	**0.7355**
Airplane	25.69	0.8556	25.80	0.8708	26.01	0.8769	26.01	0.8762	**26.11**	**0.8770**
Lake	25.58	0.8606	26.95	0.8820	26.78	0.8838	26.98	0.8844	**27.17**	**0.8870**
Milkdrop	28.85	0.9027	29.35	0.9092	29.72	0.9176	29.78	0.9170	**30.61**	**0.9216**
Girl	29.73	0.9668	30.58	0.9562	29.49	**0.9676**	29.60	0.9598	**31.16**	0.9609
Wall	23.94	0.8812	24.72	0.8903	24.63	0.8930	24.77	**0.8947**	**25.10**	0.8916
Average	25.14	0.8576	26.12	0.8733	25.86	0.8744	26.01	0.8756	**26.60**	**0.8790**

the proposed method has better vision quality and objective quality assessment value as well.

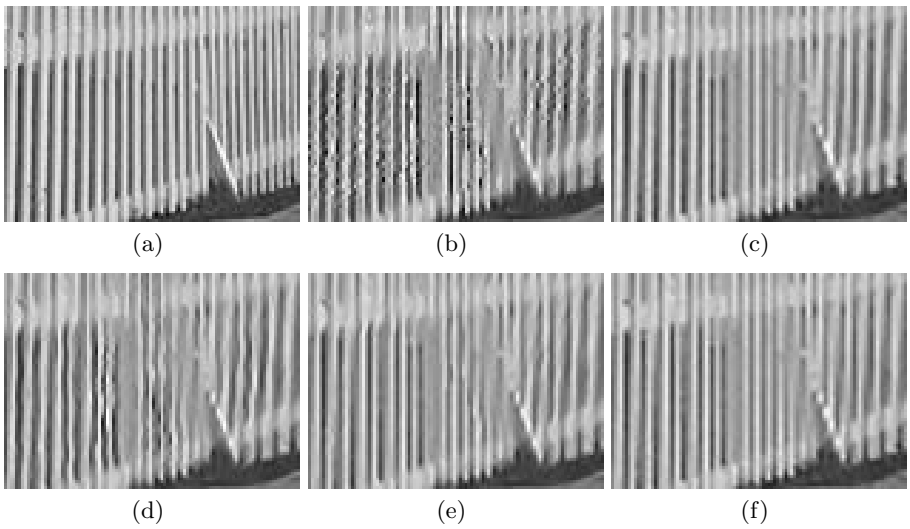

Fig. 6. Comparison on *Fence*. (a)Original image, (b)NEDI, (c)SME, (d)SAI, (e)RSAI, (f)Proposed method.

4 Conclusions

We propose an adaptive image interpolation method using rational function. The rational function is weighted and blended to remove artifacts. The edge information is used as constraints to determinate the weights adaptively. The new

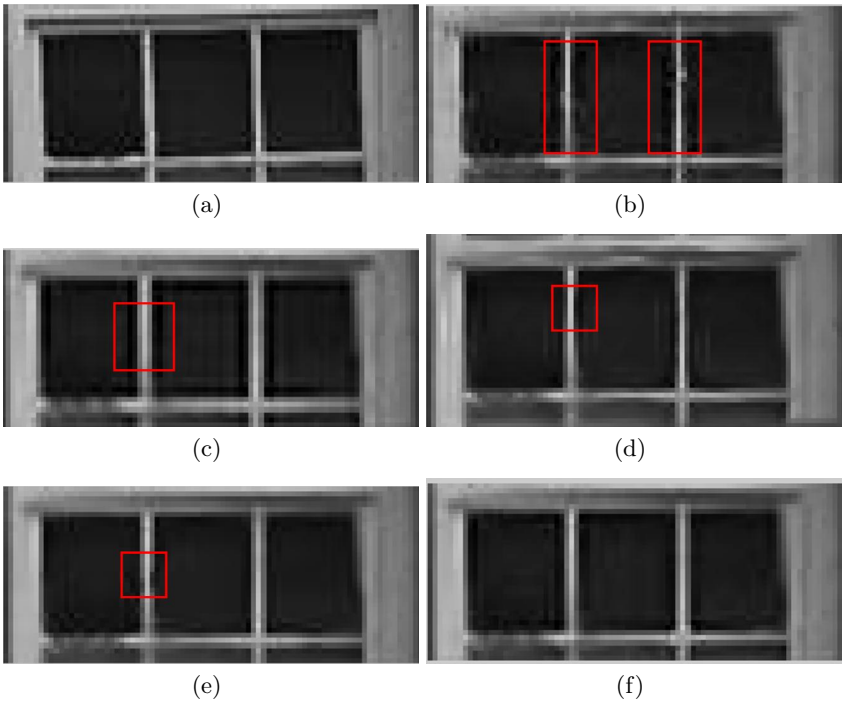

Fig. 7. Comparison on *Wall*. (a)Original image, (b)NEDI, (c)SME, (d)SAI, (e)RSAI, (f)Proposed method.

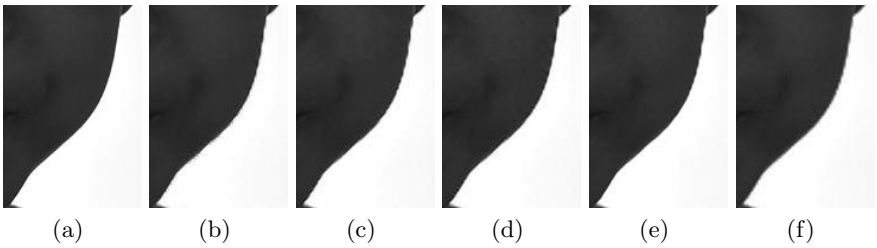

Fig. 8. Comparison on *Girl*. (a)Original image, (b)NEDI, (c)SME, (d)SAI, (e)RSAI, (f)Proposed method.

method has the advantage in that it can easily zoom the image into multiples. Our method can perform well on PSNRs and SSIMs. Furthermore, the proposed method produces clean edges and fine details.

Acknowledgement. This work was partially supported by Projects of International Cooperation and Exchanges NSFC (61020106001), National Natural Science Foundation of China under Grant 61373080, Grant 61202150, Grant 61373078.

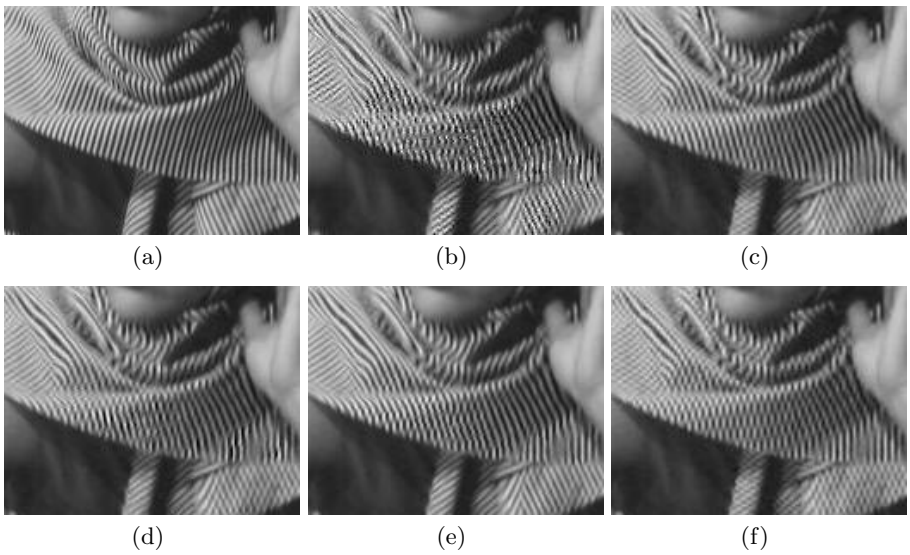

Fig. 9. Comparison on *Barbara*. (a)Original image, (b)NEDI, (c)SME, (d)SAI, (e)RSAI, (f)Proposed method.

References

1. Asuni, N., Giachetti, A.: Accuracy improvements and artifacts removal in edge based image interpolation. In: VISAPP. Volume 1. (2008) 58–65
2. Dong, W., Zhang, L., Lukac, R., Shi, G.: Sparse representation based image interpolation with nonlocal autoregressive modeling. IEEE Trans. on Image Processing **22** (2013) 1382–1394
3. Hou, H., Andrews, H.: Cubic splines for image interpolation and digital filtering. IEEE Trans Acoust, Speech and Signal and Processing **26** (1978) 508–517
4. Hu, M., Tan, J.: Adaptive osculatory rational interpolation for image processing. Journal of Computational and Applied Mathematics **195** (2006) 46–53
5. Hung, K., Siu, W.: Robust soft-decision interpolation using weighted least square. IEEE Trans. on Image Processing **21** (2012) 1061–1069
6. Key, R.: Cubic convoluion interpolation for digital image processing. IEEE Trans Acoust, Speech and Signal and Processing **29** (1981) 1153–1160
7. Li, M., Nguyen, T.: Markov random field model-based edge-directed image interpolation. IEEE Trans Image Proc **17** (2008) 1121–1128
8. Li, X., Orchard, M.: New edge-directed interpolation. IEEE Trans Image Process **10** (2001) 1521–1527
9. Mallat, S., Yu, G.: Super-resolution with sparse mixing estimators. IEEE Trans Image Process **19** (2010) 2889–2900
10. Matsumoto, S., Kamada, M., Mijiddorj, R.: Adaptive image interpolation by cardinal splines in piecewise constant tension. Optimization Letters **6** (2012) 1265–1280
11. Shezaf, N., Abramov-Segal, H., Sutskover, I., Ran, B.: Adaptive low complexity algorithm for image zooming at fractional scaling ratio. In: Proceeding of the 21st IEEE Convention of the Electrical and Electronic Engineers, IEEE (2000) 253–256

12. Sun, Q., Bao, F., Zhang, Y., Duan, Q.: A bivariate rational interpolation based on scattered data on parallel lines. J. Vis. Commun. Image R. (2013) 75–80
13. Takeda, H., Farsiu, S., Milanfar, P.: Kernel regression for image processing and reconstruction. IEEE Trans Image Process **16** (2007) 349–366
14. Thévenaz, P., Blu, T., Unser, M.: Image interpolation and resampling. In Bankman, I., ed.: Handbook of Medical Imaging, Processing and Analysis. Academic Press, San Diego CA, USA (2000) 392–420
15. Zhang, C., Wang, J.: C-2 quartic spline surface interpolation. Science in China F **45** (2002) 417–432
16. Zhang, C., Zhang, X., Li, X., Cheng, F.: Cubic surface fitting to image with edges as constraints. In: Proc IEEE Int Conf Image Processing, IEEE (2013)
17. Zhang, L., Wu, X.: An edge-guided image interpolation algorithm via directional filtering and data fusion. IEEE Trans Image Process **15** (2006) 2226–2238
18. Zhang, X., Wu, X.: Image interpolation by adaptive 2-d autoregressive modeling and soft-decision estimation. IEEE Trans Image Process **17** (2008) 887–896
19. Zhang, Y.F., Bao, F.x., Zhang, C.M, Duan, Q.: A weighted bivariate blending rational interpolation function and visualization control. Journal of Computational Analysis and Applications **14** (2012) 1303–1321